Photochemical Reaction of Ozone and Benzene: An Infrared Matrix Isolation Study

James K. Parker and Steven R. Davis*

Contribution from the Department of Chemistry, University of Mississippi, University, Mississippi 38677

Received December 18, 1998

Abstract: The photolysis of benzene/ozone mixtures in an argon matrix at 12 K with UV light of $\lambda \geq 280$ nm leads to the following products: phenol, 2,4-cyclohexadienone, benzene oxide, and butadienylketene (hexa-1,3,5-trien-1-one). The identification of butadienylketene as a product is based on deuterium isotopic shifts and agreement with density functional vibrational frequency calculations. We find an average phenol/butadienylketene branching ratio of 4.3 during the course of photolysis. This is the first report in the literature of the observation of a ketene product from the reaction of oxygen atoms with benzene.

Introduction

The reaction of benzene with oxygen (^{3}P) atoms has been the subject of several studies in the gas phase.[1−11] As a result, much data are available for this reaction including the following: specific rate constants, activation energies, the identity of reaction products, as well as proposed mechanisms. It is well-established that phenol is a primary product of this reaction. Because multiple reaction channels for this system exist there have been other products reported for this reaction. For example, Sloane[3] studied this reaction under single collision conditions in crossed molecular beams and reported two channels: formation of a long-lived complex, which rearranges to phenol, and formation of CO and a C_5H_6 hydrocarbon, presumably 3-penten-1-yne. In a subsequent study, Sibener[4] and co-workers also studied this reaction under single collision conditions in crossed molecular beams and reported two distinct reaction channels: one leading to phenol and the other to C_6H_5O and H. These workers concluded that the channel leading to CO elimination, if it occurs at all, is relatively minor. In another study[2] under multiple collision conditions, workers reported the formation of phenol and an undefined polymeric species.

Because of the fundamental significance of this reaction to the understanding of combustion processes in aromatic systems, we have undertaken a matrix isolation study of this reaction in solid argon. To our knowledge, this is the first matrix isolation study of the benzene/oxygen atom reaction. It was our goal to isolate, and characterize, via infrared spectroscopy, the primary products and intermediates of this reaction. The reaction has been studied with the following isotopomers: $C_6H_6 + {}^{16}O$, $C_6H_6 + {}^{18}O$, $C_6D_6 + {}^{16}O$, and $C_6D_6 + {}^{18}O$. As a complement to the infrared studies we have also performed density functional ab initio calculations. We have been able to identify four products of the reaction.

Experimental Procedure

Normal benzene C_6H_6 (99.8%, Aldrich) and perdeuteriobenzene C_6D_6 (99.6 atom %, Aldrich) used in these experiments were freed of relatively volatile impurities by three consecutive freeze−pump−thaw cycles at liquid nitrogen temperature. The benzene was warmed to room temperature and its vapors were expanded into an evacuated sample chamber and diluted with argon (99.995%, Air Products) to an Ar:benzene mole ratio of 300:1. Normal ozone $^{16}O-{}^{16}O-{}^{16}O$ and the isotopically pure $^{18}O-{}^{18}O-{}^{18}O$ ozone were made by passing an electric discharge, from a Tesla coil, through a sample of oxygen gas (99.996%, Air Products; ^{18}O isotope from Euriso-top, 98.01% enrichment) contained in a glass U tube which was submerged in liquid nitrogen. In this way the ozone condensed to the solid phase on the walls of the glass tube as it formed. The solid ozone was freed of residual oxygen molecules by pumping at 77 K. The purified ozone was then warmed to room temperature, expanded into a separate evacuated sample chamber, and diluted with argon to an Ar:O_3 mole ratio of 300:1. The IR spectrometer and accompanying vacuum chamber have been described in detail elsewhere.[12] The samples were co-deposited on a gold mirrored matrix support at a combined rate of 8.4 mmol/h for a total of 24.2 mmol. The matrix support was held at 12 K with a closed cycle, single stage helium refrigerator (APD Cryogenics, model DE-202). The temperature was measured at the cold plate with a gold/calomel thermocouple. All infrared spectra were recorded using a Nicolet 740 FTIR spectrometer at 1-cm^{-1} resolution. After the initial spectra were recorded, the samples were subjected to the photolyzing radiation of a 200 W Hg−Xe arc lamp (lamp model UXL 200H Hg Xe by Ushio and model A 1010 lamp housing by Photon Technology International). The radiation was filtered through a 51 mm water cell and a 580, 360, or 280 nm Hoya cutoff filter before coming in contact with the matrix sample. The temperature of the matrix sample did not rise above 14 K during any photolysis interval. All matrix spectra were successively photolyzed at precise time intervals.

The ab initio calculations were performed using the Gaussian 94 suite of programs[13] running on either a Cray C98/8512 or a Silicon Graphics Power Challenge computer. The density functional methods[14,15] of Becke, Lee, Yang, and Parr, commonly known as B3LYP

(1) Grovenstein, E., Jr.; Mosher, A. J. *J. Am. Chem. Soc.* **1970**, *92*, 3810.
(2) Bonanno, R. A.; Kim, P.; Lee, J.-H.; Timmons R. B. *J. Chem. Phys.* **1972**, *57*, 1377.
(3) Sloane, T. M. *J. Chem. Phys.* **1977**, *67*, 2267.
(4) Sibener, S. J.; Buss, R. J.; Casavecchia, P.; Hirooka, T.; Lee, Y. T. *J. Chem. Phys.* **1980**, *72*, 4341.
(5) Nicovich, J. M.; Gump, C. A.; Ravishankara, A. R. *J. Phys. Chem.* **1982**, *86*, 1684.
(6) Rotzoll, G. *Int. J. Chem. Kinet.* **1985**, *17*, 637.
(7) Ureña, A. G.; Hoffmann, S. M. A.; Smith, D. J.; Grice, R. *J. Chem. Soc., Faraday Trans. 2* **1986**, *82*, 1537.
(8) Tappe, M.; Schliephake, V.; Wagner, H. Gg. *Z. Phys. Chem.* **1989**, *162*, 129.
(9) Leidreither, H. I.; Wagner, H. Gg. *Z. Phys. Chem.* **1989**, *165*, 1.
(10) Sol, V. M.; van Drunen, M. A.; Louw, R.; Mulder, P. *J. Chem. Soc., Perkin Trans. 2* **1990**, 937.
(11) Ko, T.; Adusei, G. Y.; Fontijn, A. *J. Phys. Chem.* **1991**, *95*, 8745.
(12) Liu, L.; Davis, S. R. *J. Phys. Chem.* **1992**, *96*, 9719.

10.1021/ja984380o CCC: $18.00
Published on Web 05/05/1999

and BLYP, were used to treat electron correlation using the 6-311G-(d,p) and 6-311G(3df,3pd) basis sets,[16−19] respectively. Analytic gradients were used in the geometry optimizations with all electrons correlated. All stationary points were verified to be true minima by calculation of normal vibrational modes using the analytic second derivative method in the harmonic approximation. B3LYP/6-311G-(d,p) vibrational modes were scaled[20,21] by the factor 0.96325. Single-point calculations were carried out on the optimized B3LYP/6-311G(d,p) geometries using the 6-311G(3df,3pd) basis set. Zero-point energies were added to the electronic potential energies of each species to obtain their relative energies at 0 K.

Results

Our infrared spectra of matrix-isolated ozone[22] and benzene[23] are in good agreement with literature data for the separate species. The matrix spectra of co-deposited benzene and ozone in argon revealed no additional bands.

After 30 min of irradiation at $\lambda \geq 580$ nm no new features appeared. Irradiation at $\lambda \geq 360$ nm revealed several new bands in the 2100 cm $^{-1}$ region of the spectrum (Table 1). Other bands were also observed and their locations and assignments are given in Table 1. This table lists all product band absorptions and relative intensities resulting from $\lambda \geq 280$ nm photolysis for the four isotopomeric reactions. In each reaction, the strongest product band falls in the 2100 cm^{-1} region. Figure 1 (parts A−D) shows spectra recorded in the 2070 to 2150 cm^{-1} range after a total deposition of about 24 mmol of the gas mixtures. The only bands present in two of the spectra, before photolysis, near 2110 cm^{-1} are due to the ozone precursor. In the spectra where the ^{18}O isotope was used the ozone bands have moved out of this region and the product bands have shifted to lower wavenumber.

Gas-phase studies of the reaction of oxygen atoms with benzene have concluded that phenol is the major product of reaction. We find phenol as a product as well in the argon matrix (Table 1 and Figure 2). These bands are in good agreement with the infrared spectrum of phenol reported in the literature. Figure 2 shows the infrared spectra of product bands (standard isotopes) in the 715 to 840 cm^{-1} region.

Finally, we have identified three species produced in this reaction besides phenol. Figure 3 shows the growth kinetics of product bands when the matrix is subjected to radiation of $\lambda \geq 280$ nm. In Figure 3A is plotted the growth kinetics of phenol and a ketene product as well as the decay kinetics of ozone. (The product bands near 2120 cm^{-1} are due to a ketene, see Discussion.) Initially, both products grow in at approximately the same rate. However, at long photolysis times the rate of decay of ozone is small and the kinetic behavior of these two products is quite different. The ketene product is unstable toward the photolyzing radiation while the phenol band maintains a positive slope during the course of photolysis. This difference in kinetic behavior allowed us to assign the bands in Table 1.

The third species produced in this reaction is benzene oxide. We were able to identify this species by comparison of the product bands with the gas-phase FTIR spectrum.[24] Only the three most intense bands were observed (see Table 1). All three bands exhibit the same growth kinetics: maximum intensity at $t = 10$ min, followed by rapid exponential decay. This observation is in agreement with benzene oxide's known photoinstability: upon irradiation with photons of 320 nm $< \lambda < 480$ nm, benzene oxide isomerizes to phenol and a ketene.[25]

Figure 3B shows growth kinetics of product bands which cannot be assigned to phenol on the basis of their absorption frequencies, nor to the ketene on the basis of their kinetic behavior. The band at 1728 cm^{-1} is most likely due to a carbonyl stretch. The growth kinetics of this band suggest that it is a primary product which is unstable toward the photolyzing radiation. The bands at 1683, 1202, and 903 cm^{-1}(the 903 cm^{-1} band is not plotted in Figure 3 for clarity) have the same growth kinetics and are most likely due to the same species. Moreover, this species seems to be a secondary product as its concentration increases greatly at long photolysis times. Finally, there is a second unknown species at 774 cm^{-1} with growth kinetics that suggest it to be a primary product which is very unstable toward the radiation.

Discussion

The primary processes in ozone photolysis[26] in the 280−611 nm range are as follows:

$$O_3(^1A) \rightarrow O_2(^1\Delta_g) + O(^1D) \qquad \lambda \leq 310.0 \text{ nm} \qquad (1)$$

$$O_2(^3\Sigma_g^-) + O(^1D) \qquad \lambda \leq 411.0 \text{ nm} \qquad (2)$$

$$O_2(^1\Sigma_g^+) + O(^3P) \qquad \lambda \leq 463.0 \text{ nm} \qquad (3)$$

$$O_2(^1\Delta_g) + O(^3P)\ \lambda \leq 611.0 \text{ nm} \qquad (4)$$

When radiation is filtered through a 280 nm cutoff filter process 1 should dominate because it is spin allowed. Therefore, most of the oxygen atoms produced initially will be ^1D. Argon is known to be an effective quencher[27] of $O(^1D)$, therefore many of these atoms will go on to react as $O(^3P)$. The minimum translational energy of the oxygen atoms formed in processes 1 to 4 can be calculated from spectroscopic[27] and thermochemical[28] data. The minimum translational energy of the O (^1D) atom formed in process 1 is 39.4 kcal/mol and in process 2 is 39.3 kcal/mol. $O(^3P)$ is produced in process 3 with near zero translational energy. Processes 2 and 3 are significant only when the 360 nm filter was used. Process 4 was not significant under our experimental conditions as we could not observe ozone photolysis with radiation filtered at $\lambda \geq 580$ nm and an exposure

(13) Gaussian 94, Revision E.3, Frisch, M. J.; Trucks, G. W.; Schlegel, H. B.; Gill, P. M. W.; Johnson, B. G.; Robb, M. A.; Cheeseman, J. R.; Keith T.; Petersson, G. A.; Montgomery, J. A.; Raghavachari, K.; Al-Laham, M. A.; Zakrzewski, V. G.; Ortiz, J. V.; Foresman, J. B.; Cioslowski, J.; Stefanov, B. B.; Nanayakkara, A.; Challacombe, M.; Peng, C. Y.; Ayala, P. Y.; Chen, W.; Wong, M. W.; Andres, J. L.; Replogle, E. S.; Gomperts, R.; Martin, R. L.; Fox, D. J.; Binkley, J. S.; Defrees, D. J.; Baker, J.; Stewart, J. P.; Head-Gordon, M.; Gonzalez, C.; Pople, J. A. Gaussian, Inc.: Pittsburgh, PA, 1995.

(14) Becke, A. D. *Phys. Rev. A* **1988**, *38*, 3098.

(15) Lee, C.; Yang, W.; Parr, R. G. *Phys Rev. B* **1988**, *37*, 785.

(16) Dithcfield, R.; Hehre, W. J.; Pople, J. A. *J. Chem. Phys.* **1971**, *54*, 724.

(17) Hariharan, P. C.; Pople, J. A. *Theo. Chim. Acta* **1973**, *28*, 213.

(18) McLean, A. D.; Chandler, G. S. *J. Chem. Phys.* **1980**, *72*, 5639.

(19) Krishnan, R.; Binkley, J. S.; Seeger, R.; Pople, J. A. *J. Chem. Phys.* **1980**, *72*, 650.

(20) This scaling factor was empirically derived in our laboratory by recording the infrared spectrum of dimethylketene in solid argon and dividing the asymmetric ketene stretching frequency by the B3LYP/6-311G-(d,p) infrared frequency of this mode.

(21) Scott, A. P.; Radom, L. *J. Phys. Chem.* **1996**, *100*, 16502.

(22) Andrews, L.; Spiker, R. C., Jr. *J. Phys. Chem.* **1972**, *76*, 3208.

(23) Brown, K. G.; Person, W. B. *Spectrochim. Acta, Part A* **1978**, *34A*, 117.

(24) Klotz, B.; Barnes, I.; Becker, K. H.; Golding, B. T. *J. Chem. Soc., Faraday Trans.* **1997**, *93*, 1507.

(25) Jerina, D. M.; Witkop, B.; McIntosh, C. L.; Chapman, O. L. *J. Am. Chem. Soc.* **1974**, *96*, 5578.

(26) DeMore, W. B.; Raper, O. F. *J. Chem. Phys.* **1966**, *44*, 1780.

(27) Okabe, H. *Photochemistry of Small Molecules*; John Wiley and Sons: New York, 1978.

(28) Wagman, D. D. *J. Phys. Chem. Ref. Data* **1982**, *11*, Suppl. 2, 1.

Table 1. Absorptions (cm^{-1}) Observed in the Reaction of Oxygen Atoms with Benzene at $\lambda \geq 280$ nm

$^{16}O_3$/benzene-H_6/Ar O_3 58% photolyzed	rel intensity	$^{18}O_3$/benzene-H_6/Ar O_3 50% photolyzed	rel intensity	$^{16}O_3$/benzene-D_6/Ar O_3 53% photolyzed	rel intensity	$^{18}O_3$/benzene-D_6/Ar O_3 69% photolyzed	rel intensity	assignment
3633.2	10.1	3620.2	10.4	2682.6	6.7	2666.0 2665.1	6.8	phenol
2133.4[a] 2124.7[a] 2121.4[a] 2116.3[a]	100	2105.3 2097.5 2096.8 2094.5 2093.4	100	2129.5 2125.8 2121.2 2118.7 2117.2	100	2102.6 2099.8 2098.0 2094.6 2091.7 2090.4 2089.6 2084.9	100	BDK
1728.6	1.6	1694.8 1693.4 1693.8-min	2.4	1718.6	2.5	1674.1	0.5	2,4-cyclohexadienone
1683.2 1679.0	0.9	1672.0	1.2			1650.7	0.3	unknown 1
1623.7	2.1			1586.1 1583.5	2.5	1586.5 1585.8 1585.0 1583.6	4.2	phenol
1610.4	6.0	1609.7	9.0	1573.5 1572.3 1570.4 1569.3	7.6	1571.0 1569.2 1567.7 1565.3	11.2	phenol
1603.8[a] 1601.9[a]	18.2	1603.5 1601.1	22.7	1399.5 1398.1 1397.1	26.9	1399.8 1397.4 1394.5 1392.4	24.3	phenol
1544.7	0.5							?
1504.6[a] 1501.6[a]	12.6	1504.5 1500.1	11.9	1356.5	0.4	1354.3	1.1	phenol
1472.8 1471.2	6.3	1471.5 1469.9	5.5	1294.4 1293.0	2.1	1294.0 1292.7 1290.8	1.9	phenol
1344.3[a]	5.8	1343.0 1341.0	5.9	1270.7	4.8	1268.1	17.9	phenol
1328.5	1.4	1327.6	1.2	1191.1 1183.1	16.3	1176.6 1173.3	11.2	phenol
		1268.1	5.0					?
		1256.9	1.9					?
1262.7 1255.9	16.2	1250.8 1249.1 1248.4	6.7	1101.0	3.2			phenol
1248.1	0.2							benzene oxide
1202.2 1199.7	2.4	1200.0	2.7					unknown 1
1177.0[a]	20.2	1173.0 1170.1	13.6	1062.0 1060.3	1.5	1058.9 1057.7	2.0	phenol
1170.4 1168.8	2.4	1168.3	1.3					phenol
1160.1 1158.7	1.4	1158.8 1157.5	2.1	960.6 959.6	0.3			phenol
1152.8[a] 1149.9[a]	8.7	1150.5 1148.4	12.6	904.5	16.5	896.1 895.3 894.5	14.5	phenol
1081.4[a] 1079.8[a]	1.6							benzene oxide
1074.0[a] 1071.1[a]	1.4	1073.8 1070.7	1.6	878.0 877.2	2.9	866.6	0.9	phenol
		1027.2 1025.5	1.9					?
1000.6	0.9			755.4 754.7	1.9	754.6	1.7	phenol

Table 1. continued

$^{16}O_3$/benzene-H_6/Ar O_3 58% photolyzed	rel intensity	$^{18}O_3$/benzene-H_6/Ar O_3 50% photolyzed	rel intensity	$^{16}O_3$/benzene-D_6/Ar O_3 53% photolyzed	rel intensity	$^{18}O_3$/benzene-D_6/Ar O_3 69% photolyzed	rel intensity	assignment
987.9	0.9							?
942.3	1.6	942.2 940.0	1.0					?
902.7 899.9 898.3	2.8	904.9 903.1 900.0 898.3	3.3					unknown 1
882.4 880.7	1.8	882.2 880.5	1.9	752.0 750.6	2.6	745.7 744.5	2.6	phenol
826.0	1.4			624.6	0.8	624.4	0.5	phenol
817.3[a] 811.8[a]	3.8	804.0 802.0	4.1	586.9	0.4			phenol
784.0	1.0	783.2	0.5					?
773.7	1.7	769.7	1.1					unknown 2
752.3	15.6	752.7 751.9	13.9	551.5 550.4	6.1	551.2 550.2	5.6	phenol
738.2[a]	4.2	737.7	2.3					benzene oxide
724.2	1.0	724.2	0.9					BDK
688.9[a] 687.4[a]	5.1	689.2 687.2	7.6	504.0	1.2			phenol
528.6	0.4							phenol
504.9[a]	2.4	503.8	1.8					phenol
		502.5	1.2					?
		494.0	0.3					?
		485.3	0.5					?

[a] *a* indicates band was observed at $\lambda > 360$ nm and t = 30 min. The 360 nm filter was used only in the reaction of standard isotopes.

time of 30 min. A recent study[29] of the photochemistry of ozone in argon matrices suggests that once an O(^{1}D) atom escapes the matrix cage where it is formed it moves easily through the argon lattice because of a short-range attractive interaction between argon and O(^{1}D). The O(^{3}P) atom experiences a long-range repulsive interaction with the argon lattice. Molecules such as benzene, however, are unable to diffuse through an argon matrix at 12 K. In this study we have assumed that O(^{1}D) can diffuse through the matrix (and to a lesser degree triplet atomic oxygen) before reacting with benzene.

Referring to Table 1 and Figure 1, we find that the most intense product bands occur in the 2100 cm^{-1} region of the spectrum. Considering the reaction of the normal isotopomers, four intense product bands at 2133.4, 2124.7 and 2121.4, and 2116.3 cm^{-1} are easily seen in Figure 1A. Upon substitution with ^{18}O these bands shift to 2105.3, 2096.8, and 2094.5 cm^{-1}. In compounds of the elements C, H, and O, the only functional group with an intense infrared absorption[30] in this spectral region is the ketene group, $R_2C{=}C{=}O$. For a given infrared mode, the square of the frequency ratio gives the reduced mass ratio in the diatomic approximation. The asymmetric stretch of a ketene group can be modeled as a vibration of the central carbon atom against stationary oxygen and carbon atoms on either side; therefore, $\mu_{18}/\mu_{16} = 1.020$. Taking the square of the ratio (ν_{16}/ν_{18}), for the bands listed above, yields the following: $(2133.4/2105.3)^2 = 1.027$, $(2124.7/2096.8)^2 = 1.027$, and $(2121.4/2094.5)^2 = 1.026$. (The 2116.3 cm^{-1} mode is rather poorly defined and we were unable to assign it to a band in Figure 1B.) Since there is reasonable agreement with the reduced mass ratio in the diatomic approximation, we conclude that the measured shifts are consistent with the ketene functional group.

In order for a molecule with a ketene functional group to form from the reaction of benzene and oxygen atoms, the benzene ring must open. Since no evidence for smaller fragments is present in the spectra, we will only consider ketene molecules with the empirical formula C_6H_6O as possible products. Although the reaction is exothermic, and consequently the initial product should be formed in an excited vibrational state, condensed phases favor collisional deactivation over fragmentation.

Two possible structures of the ketene product are

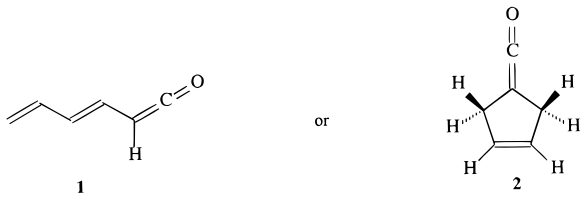

1 **2**

We can readily decide between these two structures on the basis of the isotopic shifts in their infrared spectra. Referring to Table 1 and Figure 1A, there is an intense ketene band at 2124.7 cm^{-1}. Upon substituting all hydrogen atoms with deuterium (Figure 1C) this band shifts to 2118.7 cm^{-1}, a shift of -6.0 wavenumbers. Table 2 lists the B3LYP/6-311G(d,p) calculated frequencies for structures **1** and **2**. For structure **1**, the perhydrogen compound has an asymmetric stretch at 2129.0 cm^{-1} while the perdeuterium compound has the corresponding mode at 2123.5 cm^{-1}. The deuterium isotope has lowered the frequency of this mode by 5.5 cm^{-1}. This calculation is in good agreement with

(29) Benderskii, A. V.; Wight, C. A. *J. Chem. Phys.* **1994**, *101*, 292.

(30) Daimay, L.-V. *The Handbook of Infrared and Raman Characteristic Frequencies of Organic Molecules*; Academic Press: Boston, 1991.

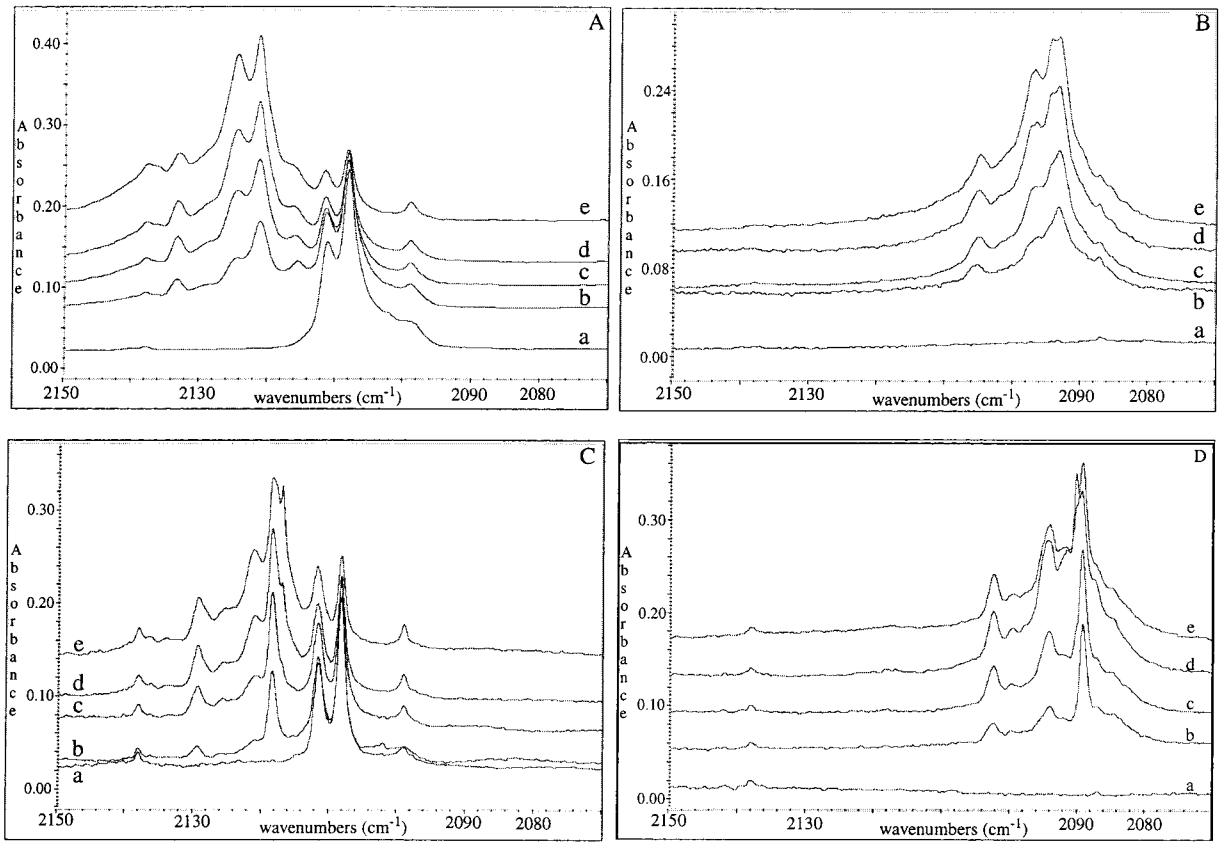

Figure 1. Infrared spectra of product bands from 280 nm photolysis in the 2070−2150 cm^{-1} region for the four isotopomeric reactions: (A) ^{16}O, ^{1}H, (B) ^{18}O, ^{1}H, (C) ^{16}O, ^{2}H, and (D) ^{18}O, ^{2}H (a) spectra before photolysis and after (b) 10 min, (c) 30 min, (d) 60 min, and (e) 120 min of Hg arc photolysis.

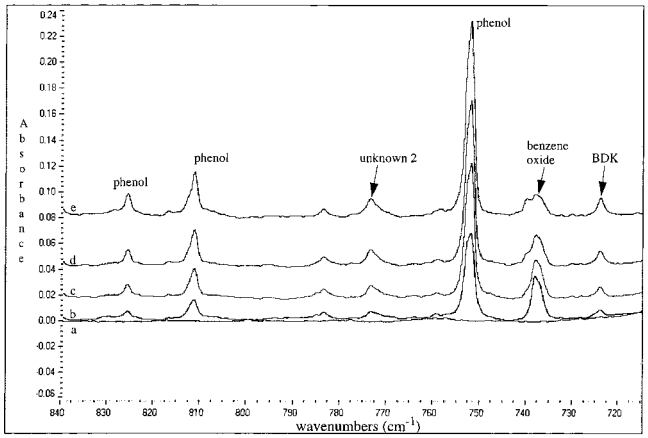

Figure 2. Infrared spectra in the 715−840 cm^{-1} range for the reaction of ^{16}O and benzene-H_6: (a) spectrum before photolysis and (b) 10 min, (c) 30 min, (d) 60 min, and (e) 120 min after photolysis.

the experimental observation. In structure **2**, the perhydrogen compound exhibits the ketene asymmetric stretch at 2129.2 cm^{-1}. Substituting all hydrogens with deuterium we find that the mode splits, and shifts to 2133.0 and 2096.5 cm^{-1}, corresponding to frequency changes of +3.8 and −36.5 cm^{-1}. The reason for the splitting of this mode is that the asymmetric ketene stretch has become strongly coupled with a C−D symmetric stretching mode in this isotopomer, causing the band to split and shift to higher and lower frequencies. However, this behavior is not observed experimentally, and consequently structure **1** is assigned as the structure of the ketene product. For the rest of the paper we will refer to **1** as butadienylketene (BDK). (The IUPAC name for BDK is hexa-1,3,5-trien-1-one).

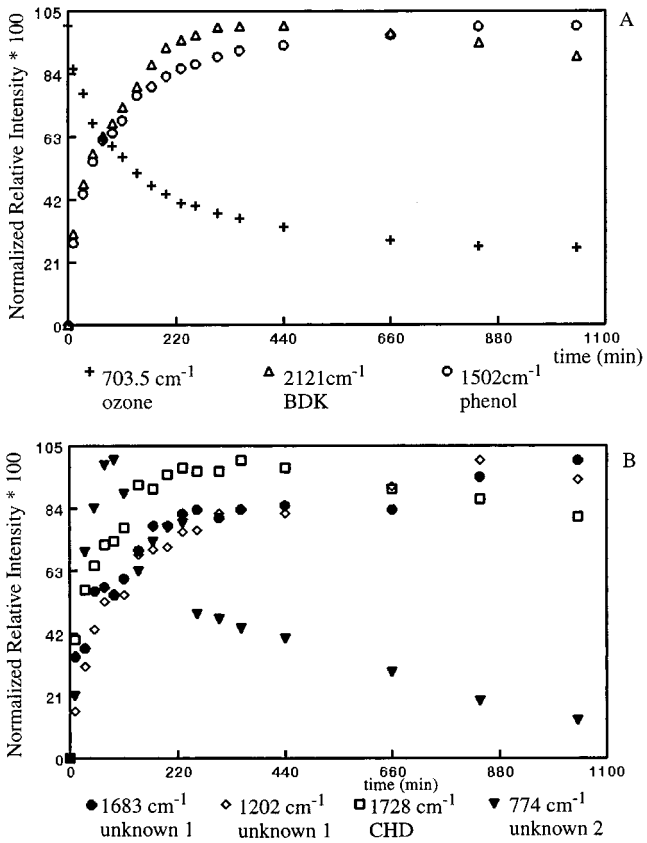

Figure 3. Photolysis time dependence of product band intensities from the $^{16}O_3$/benzene-H_6 photolysis reaction: (A) phenol and BDK product bands and (B) 1,3-cyclohexadienone and unidentified product bands.

Table 2. B3LYP/6-311G(d,p) Frequencies (cm^{-1}) of Ketene Asymmetric Stretch for Structures **1** and **2**

	freq		
structure	(^{12}C,^{16}O,^{1}H)	(^{12}C,^{16}O,^{2}H)	shift
1	2129.0	2123.5	−5.5
2	2129.2	2133.0	+3.8
		2096.5	−32.7

Table 3. B3LYP/6-311G(3df,3pd) // B3LYP/6-311G(d,p) Relative Energies and Frequencies of Products from the Benzene/Oxygen Atom Reaction

species	rel energy (kcal/mol)	asym str freq (cm^{-1})
(*E*)-BDK-*t*,*t*	−65.4	2129.0
(*E*)-BDK-*c*,*t*	−63.7	2122.9
(*E*)-BDK-*t*,*c*	−61.7	2127.9
(*E*)-BDK-*c*,*c*	−60.0	2123.2
(*Z*)-BDK-*t*,*t*	−64.0	2129.5
(*Z*)-BDK-*c*,*t*	−62.0	2117.1
(*Z*)-BDK-*t*,*c*	−60.5	2128.4
(*Z*)-BDK-*c*,*c*	−58.0	2120.4
2,4-cyclohexadienone	−81.9	NA
phenol	−100.8	NA
benzene + O(^{3}P)	0	NA

To our knowledge, butadienylketene has never been reported as a product of the benzene/oxygen atom reaction. However, the reaction has precedent. Capponi et al.[31] report that photolytically generated 2,4-cyclohexadienone (CHD) in water undergoes secondary photolysis to form butadienylketene. This observation provides insight into the mechanism of the reaction. Our postulated mechanism is given as

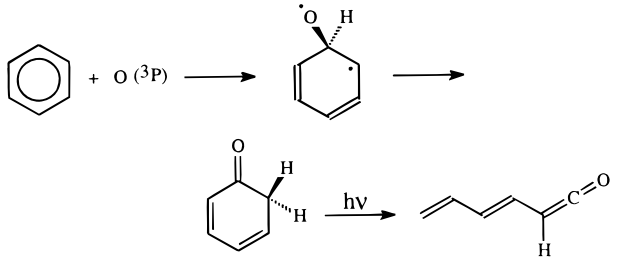

The first step in the mechanism is the reaction with triplet state oxygen atoms to form a benzene−oxygen biradical complex. Initially, this complex must be formed in the triplet state to conserve spin. This structure rapidly decays to cyclohexadienone by hydrogen atom migration and intersystem crossing. The cyclohexadineone now absorbs a photon and the carbonylcarbon−methylene carbon single bond cleaves homolytically to form butadienylketene. This mechanism is further supported by the data in Figure 3 which show that cyclohexadienone is unstable toward the photolyzing radiation. Jerina and McIntosh[25] have postulated a similar mechanism for the photorearrangement of benzene oxide in solution at 77 K. Klotz[24] and co-workers have also referred to this mechanism in their investigation of the gas-phase photorearrangement of benzene oxide.

There are eight possible conformational isomers of butadienylketene. Their computed relative energies and ketene asymmetric stretching frequencies are given in Table 3. The *E*/*Z* label has its usual meaning and refers to the orientation of the molecule about the central C−C double bond. The orientation of each C−C single bond is designated as either trans or cis with the letters *t* or *c*. The first letter refers to the orientation of the C−C single bond adjacent to the ketene group; the second letter refers to the remaining C−C single bond. In Table 3, the average relative energy of the BDK isomers (as compared to the energy of the unreacted benzene and oxygen ^{3}P atom) is −61.9 kcal/mol with a standard deviation of ±2.4 kcal/mol. Because the relative energies of the isomers are closely grouped, it is not unreasonable to assume that most or all of these isomers have been trapped in the matrix reaction. There are four discernible absorptions in the ketene region for products with standard isotopes (Table 1). It is likely that each of these four absorptions is due to one or more of the conformational isomers of butadienylketene. The range of deviation among the calculated frequencies is 12.4 wavenumbers. Experimentally, we find a range of 17.1 wavenumbers. For products with the ^{18}O and ^2H isotopes, eight absorptions are observed in the ketene region. These observations lend support to the possibility that all eight conformational isomers of butadienylketene are trapped in the matrix.

Scheme 1

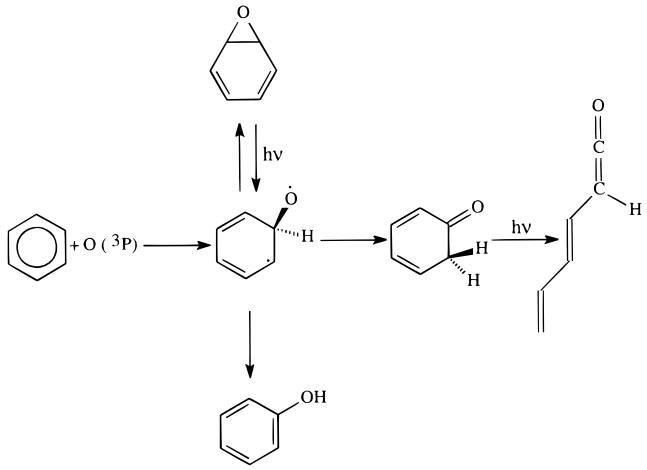

To investigate the possibility that the multiple ketene absorptions are due to the same species trapped in different lattice sites, each matrix was annealed to 27 K for 1 min and then an infrared spectrum was taken. There was no change in the peak positions, supporting each absorption being due to a unique conformation.

Further examination of Table 3 reveals that the relative energy of cyclohexadienone is approximately midway between the average relative energies of the butadienylketene isomers and phenol. According to our postulated mechanism, the BDK product forms from photolysis of the intermediate cycohexadienone. We have observed a product absorption in the carbonyl region of the spectrum at 1728.6 cm^{-1}. The reduced mass ratio of the carbonyl functional group is $\mu_{18}/\mu_{16} = 1.050$ in the diatomic approximation. From Table 1 the ratio of the squares of the ^{16}O, ^1H and ^{18}O, ^1H modes is $(1728.6/1693.8)^2 = 1.042$. Also, the ratio of the squares of the ^{16}O, ^2H and ^{18}O, ^2H modes is $(1718.6/1674.1)^2 = 1.054$. Since there is reasonable agreement of the observed reduced mass ratio with the approximated ratio, and because this band falls within the region of the spectrum characteristic of carbonyls, we assign this band to 2,4-cyclohexadienone.

A summary of the matrix reactions is given in Scheme 1. It is noted that the possibility exists that some of the phenol product may have been formed by insertion of O(^{1}D) into a C−H bond of benzene. The branching ratio, [phenol]/[BDK], can be determined from Beer's law:

(31) Capponi, M.; Gut, I.; Wirz, J. *Angew. Chem., Int. Ed. Engl.* **1986**, *25*, 344.

$$[C]b = A/I$$

where A is the integrated absorbance, I is the band intensity, and b is the path length. The experimentally determined intensity of the phenol ν_{19} mode (1504.6 and 1501.6 cm^{-1} in argon matrix) is given as 36 km/mol by Brownlee[32] and co-workers. Our calculated BLYP/6-311G(3df,3pd) intensity of the asymmetric stretching mode of butadienylketene is 1221 km/mol. Porezag[33] and Nascimento[34] have reported that this density functional method allows for accurate calculation of infrared intensities. Indeed, we find a calculated intensity of 35.70 km/mol for the phenol ν_{19} mode at this level; the resulting error in the calculation is only 0.8%.

Figure 4 plots the phenol/BDK branching ratio as a function of photolysis time. The value of the ratio lies in the range 4.1 to 4.5 from $t = 10$ to 440 min. During this period the average branching ratio is 4.3. Photolysis at times greater than 440 min causes the ratio to increase in a seemingly linear fashion. This can be explained by the observation that phenol is stable toward photolyzing radiation of $\lambda \geq 280$ nm while BDK is not (Figure 3). The photolysis of BDK must lead to the formation of a product with secondary growth kinetics. We now postulate that unknown 1 is the product of the photolytic decay of BDK.

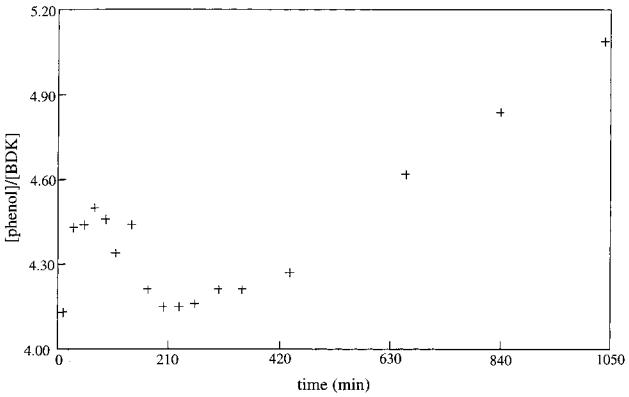

Figure 4. Plot of the phenol/BDK concentration ratio as a function of photolysis time.

Conclusions

The photochemical reaction of benzene and ozone in a solid argon matrix at 12 K yields the following products: phenol, 2,4-cyclohexadienone, benzene oxide, and butadienylketene. Butadienylketene is formed by photolysis of cyclohexadienone. We find an average branching ratio for the formation of phenol and BDK of 4.3. The average relative energy of a BDK molecule is calculated to be -61.9 ± 2.4 kcal/mol. The discovery of this photochemical reaction has possible implications in the atmospheric chemistry of benzene.

Acknowledgment. Partial support from the National Science Foundation through NSF EPSCOR (OSR-9452857), NSF (CHE-9512473) as an equipment grant, and the Office of Naval Research (N00614-93-1-0079) is gratefully acknowledged. We also thank the Mississippi Center for Supercomputing Research for computer time.

JA984380O

(32) Brownlee, R. T. C.; Cameron, D. G.; Topsom R. D.; Katritzky, A. R.; Sparrow, A. J. *J. Mol. Struct.* **1973**, *16*, 365.

(33) Porezag, D.; Pederson, M. R. *Proc. Sci. Technol. At. Eng. Mater.* **1996**, 483.

(34) Nascimento, I. C.; DeOliveira, A. E.; Bruns, R. E. *Spectrochim. Acta, Part A* **1998**, *54A(6)*, 831.